The Effect of Ambient Stratification and Moisture on the Motion of Atmospheric Undular Bores

N. ANDREW CROOK*

Geophysical Fluid Dynamics Program, Princeton University, Princeton, NJ 08542

ABSTRACT

A numerical model is used to examine the effects of ambient stratification on the behavior of an atmospheric undular bore. It is shown that stratification reduces the amplitude of the disturbance at low levels by allowing energy to propagate upward. This reduction of amplitude can be inhibited by specifying winds opposing the wave motion in the middle and upper troposphere. Mean observations in the region where the Morning Glory is prevalent support this result.

The effects of moisture are also examined. If condensation does not occur, moisture increases the disturbance amplitude by reducing, through virtual temperature effects, the stability of the atmosphere. However, if condensation occurs, the wave amplitude is decreased compared with a dry atmosphere with the same effective stability. Finally, it is shown that cloud formation increases the wavelength of the disturbance.

1. Introduction

In an earlier paper (Crook and Miller, 1985; hereafter referred to as CM), the behavior of atmospheric undular bores was studied with the aid of a mesoscale numerical model. The atmospheric profiles used in that work exhibited a layer of high stratification near the ground (hereafter referred to as the stable layer) with a much deeper, neutrally stratified, layer above. A density current was then allowed to propagate into the stable layer and, as long as the characteristics of the density current and stable layer were chosen correctly, an undular bore would propagate ahead of the current. The model fields were then compared with observations of an atmospheric bore, the Morning Glory of northern Queensland (see Clarke et al., 1981) and encouraging agreement found.

In the present work, the effects of stratification above the stable layer are examined. As discussed briefly in CM, this upper level stratification allows waves to propagate above the stable layer and energy to be radiated upwards. In fact, for typical values of atmospheric stratification, energy radiation can be very important and can reduce the lifetime of an undular bore to a few minutes (see Clarke et al., 1981). In the work that follows, we shall attempt to elucidate one method for inhibiting the radiation of energy away from the stable layer.

The effects of moisture on the motion of an undular bore will then be examined. Although "dry" Morning Glorys have been recorded, they usually occur with one, two or more cloud bands. It has been suggested that these clouds, by releasing condensational energy, may increase the wave amplitude (see Clarke et al., 1981). However, as will be seen, precisely the opposite effect occurs.

2. Results

a. The numerical model

The numerical model used is a two-dimensional, nonhydrostatic, primitive equation model with pressure as a vertical coordinate. The model is based on that described in Miller and Pearce (1974). In the present study some additional changes are made to facilitate the modeling of a density current and these are listed in CM.

A definition sketch of the numerical domain showing the density current and stable layer is given in Fig. 1. After the current has interacted with the stable layer, a Galilean transformation is applied in the horizontal to keep the disturbance inside the model domain. In experiment 1, the change in velocity is -7.2 m s^{-1} and in succeeding experiments, -8.5 m s^{-1}.

A damping layer is incorporated at the top of the domain in all of the simulations described after the first. This layer is included by adding to each prognostic equation a term of the form

$$K(p)[f_s - f],$$

where $K(p) = 2\pi/T(p)$, $T(p)$ is the profile of relaxation period, and the subscript s represents the initial environmental profile. In the lower two-thirds of the model,

* Previous Affiliation: Atmospheric Physics Group, Imperial College, London, SW7 2BZ, U.K.

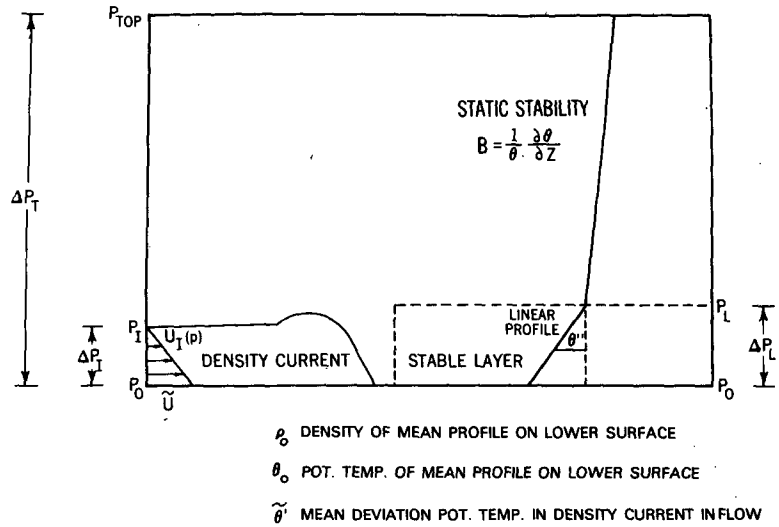

FIG. 1. Definition sketch of density current and stable layer showing the notation to be used.

$K(p)$ is set to zero, then increased linearly above that to a value $K_{TOP} = 2(2\pi/T_M)$ at the top of the model. Several experiments were performed to find the optimum value of the mean relaxation period T_M giving the smoothest decrease of the fields in the damping layer. The final value chosen was $T_M = 20$ minutes, which is of the same order of magnitude as the period of gravity waves in the upper layer.

In CM, the numerical results were presented in nondimensional form by dividing the fields by characteristic scales in the flow. This made it easier to compare the numerical results with analytical models of undular bores. In the present work, where comparison is made solely with real atmospheric observations, all fields are presented in dimensional form.

b. Stratified upper layer

1) NO SHEAR

The most common parameter used to describe the stratification of an atmosphere is the Brunt-Väisälä frequency

$$N = \left(\frac{g}{\theta}\frac{\partial\theta}{\partial z}\right)^{1/2}.$$

Closely related is the static stability $B = \theta^{-1}\partial\theta/\partial z$.

In the first simulation to be considered, a constant value of the static stability will be prescribed throughout the upper layer. For an atmosphere with a constant static stability B, the variation of potential temperature θ with height is given by

$$\theta = \theta_0 e^{Bz},$$

where θ_0 is surface potential temperature. Using the hydrostatic equation, it is then easy to show that the variation of potential temperature with pressure is

$$\theta = \theta_0 \Big/ \left\{1 + B\theta_0 C_p g^{-1}\left[\left(\frac{p}{p_0}\right)^{\kappa} - 1\right]\right\}$$

where p_0 is the surface pressure and $\kappa = R/C_p$.

Atmospheric soundings before and after the passage of a Morning Glory reveal that above the low-level stable layer (and up to about 4 km), the atmosphere is only weakly stratified with an average static stability of approximately 5.0×10^{-6} m^{-1}. At about 4 km, there often exists a temperature inversion (see Smith and Morton, 1984) and above this level the stratification returns to a more typical subtropical value of $B = 1.2 \times 10^{-5}$ m^{-1}.

In the first simulation to be discussed (experiment 1), the static stability is taken as 5.0×10^{-6} m^{-1} throughout the atmosphere above the stable layer. This simplification is made so that the effect of gravity waves in the upper layer can be more easily studied.

The remaining characteristics of the model (e.g., depth and temperature difference of density current and stable layer) are the same as for experiment 3 of CM. The grid spacing, time step and domain size in dimensional units are

$$\Delta x = 790 \text{ m},$$
$$\Delta p = 15 \text{ mb},$$
$$\Delta t = 30 \text{ seconds},$$
$$\text{Domain size} = 72 \text{ km} \times 600 \text{ mb}.$$

In Fig. 2, the vertical velocity and deviation potential temperature fields are shown at a real time of $t = 360$ minutes. Comparing these fields with Figs. 4 and 6 of

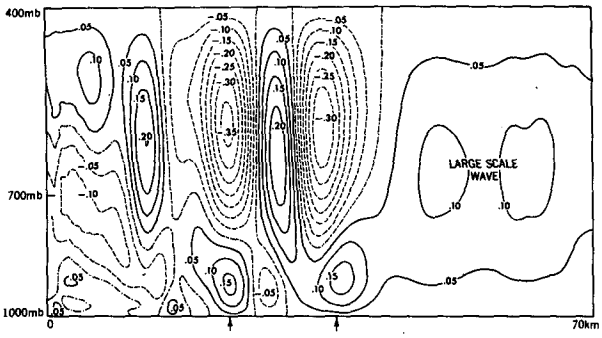

FIG. 2(a). Vertical velocity field for experiment 1 at $t = 360$ minutes (in m s^{-1}). Arrows indicate the possible position of an undular bore type disturbance.

CM, it is clear that the addition of stability to the upper layer has had a significant effect on the overall flow. (To compare the fields, the vertical velocity field of CM needs to be multiplied by a velocity scale of 8.0 m s^{-1} and potential temperature field by 3.0°C.) First, there exists a large region of upward velocity (with a maximum vertical velocity of 0.12 m s^{-1}) which has propagated ahead of the main disturbance and is interacting with the right-hand boundary. This disturbance, which has been labeled "large-scale wave," takes the form of a gravity wave propagating throughout the depth of the atmosphere and trapped by the upper and lower pressure surfaces.

Downwind of the large-scale wave there exists a disturbance (indicated by arrows) propagating with a velocity of 9.0 m s^{-1} on the lower stable layer. However, the maximum vertical velocity in this wave is only 0.18 m s^{-1}. Furthermore, in the upper layer, there exists downward velocity of even greater magnitude.

The wave at upper levels is clearly strongly influenced by the upper boundary. To minimize any wave reflection that might occur, the upper boundary in the succeeding experiments is moved to 100 mb and the damping layer, described in section 2.1, specified above 400 mb.

2) INCLUSION OF SHEAR

Clearly, the addition of stratification to the upper layer has had a profound effect on the overall flow. If the wave at lower levels in Fig. 2 is identified as a Morning Glory type disturbance, then the addition of stratification has decreased the amplitude of the disturbance by an order of magnitude compared with observations and the disturbances described in CM.

The appearance of large vertical velocities above the stable layer suggests that energy is being transmitted into the upper layers in the manner described by Eliassen and Palm (1961). To produce a disturbance with a large amplitude near the ground, it is clearly necessary to inhibit this radiation of energy upwards. Scorer (1949) showed that energy can be trapped at low levels when the parameter

$$l^2 = \frac{gB}{(U-c)^2} - \frac{U''}{(U-c)}$$

(commonly called the Scorer parameter) decreases with height; (c is the wavespeed). If the curvature term is ignored for the present moment, then the Scorer parameter will decrease with height if either the static stability B decreases in the upper layer or the ambient wind relative to the wave, $U - c$, increases. The first possibility of a reduced static stability moves the atmosphere towards the neutral state examined in CM. However, the static stability used in experiment 1 ($B = 5.0 \times 10^{-6}$ m^{-1}) is commonly observed when Morning Glorys occur, and it is difficult to justify decreasing the stability further.

However the second possibility of opposing winds in the upper layer can be justified on the basis of climatic data. Although no radiosonde measurements exist for Burketown, Queensland (where the Morning Glory observational network is usually based), they do exist for Mt Isa (300 km south of Burketown) and Townsville (800 km east). In Fig. 3, the monthly mean observations for September averaged over five years (1978–82) are plotted. The month of September is chosen as it is one of the months of maximum frequency of Morning Glorys (Clarke et al., 1981). (The observations are taken from *WMC, Monthly Climatic Data for the World,* published by NOAA). Plotted is the west–east component (there is very little amplitude in the north–south component, apart from that due to weak southeasterly trade winds below 4 km) and the potential temperature for both Mt Isa and Townsville. As can be seen, there is very little variation in the observations from the two localities, which suggests that similar conditions occur in the Burketown area.

Perhaps the most striking feature of the observations is the strong westerly jet, reaching a velocity of almost 30 m s^{-1} centered about 250 mb. As the profile is the five-year average of a monthly mean, the jet on any particular day could be considerably stronger.

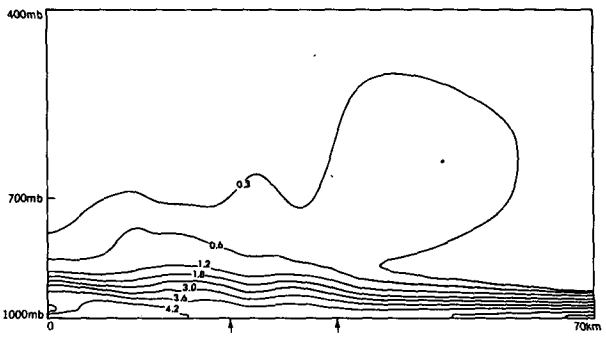

FIG. 2(b). As in 2a except for deviation potential temperature (°C).

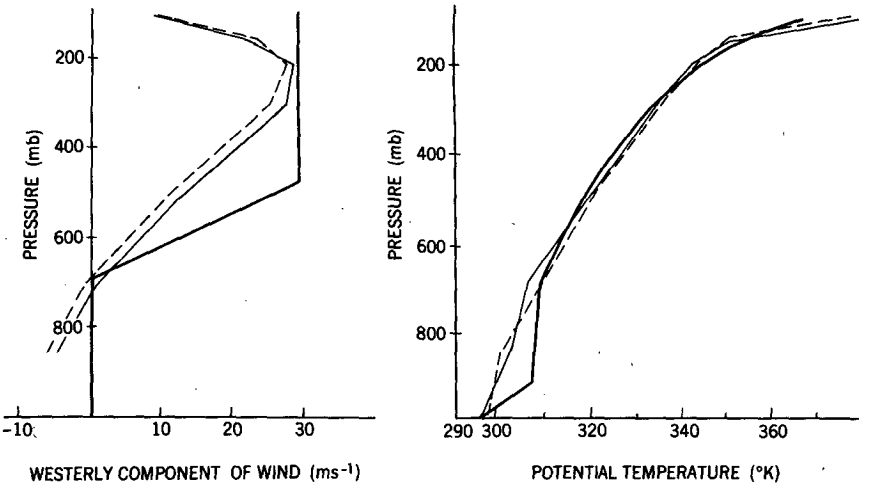

FIG. 3. Five-year average of the September monthly mean for Mt Isa (thin, continuous line) and Townsville (dashed line). Also depicted are the profiles used in experiment 2 (thick continuous line).

The westerly jet evident in Fig. 3 is clearly an important feature of the atmospheric environment of northern Queensland. If the jet is included in the model, then, to remain consistent, it is also necessary to specify a potential temperature profile which is closer to the observed mean profile than that previously used. For this reason, a stratification similar to the Mt Isa and Townsville mean observations is used above 650 mb, while the profile observed at Burketown below 4 km is retained over that layer. (This simulation will be called experiment 2.) To test the effect that the stronger stratification *alone* has on the model simulations, an experiment was run with no upper level jet in the environment. Not surprisingly, more energy was transmitted into the upper layer and, consequently, the amplitude of the disturbance at low levels was further decreased.

The velocity and potential temperature profiles to be used in experiment 2 are shown in Fig. 3. The velocity profile is chosen so as to represent a day on which the upper level jet is somewhat stronger than the mean. The stratification in the stable layer is slightly increased in this experiment. The potential temperature difference across the stable layer is increased to 10°C, which was the observed difference on 4 October 1979 (Clarke et al., 1981).

Before examining the results of a simulation using the velocity and potential temperature structure shown in Fig. 3, it should be noted that the velocity profile has two singularities in the curvature term $U''/(U - c)$ of the Scorer parameter. When the velocity profile is finite differenced in the numerical model, these singularities are removed and become levels of large but finite curvature. Furthermore, the mixing terms which are included in the model tend to smooth out the velocity profile and hence reduce the value of the curvature term. The importance for wave energy propagation of the thickness of the layer, over which the curvature term is large, will be discussed later.

The Richardson number for the profiles shown in Fig. 3. has also been calculated. The minimum Ri number is 0.37 which occurs in the section of the shear layer which is only weakly stratified (static stability $B = 5.0 \times 10^{-6}$ m^{-1}). Hence, the shear layer is stable to Kelvin–Helmholtz waves.

In Fig. 4, the vertical velocity and deviation potential temperature fields at $t = 240$ min are shown. The inclusion of the upper level jet has clearly had a significant effect on the overall flow pattern. First, there is no large-scale wave ahead of the major disturbance. The wave on the lower layer now decays with height, with no large downward velocities above. Furthermore, the amplitude of this wave has significantly increased, giving maximum vertical velocities of approximately 0.8 m s^{-1}. (The vertical velocity slowly increases towards the end of the simulation; at $t = 180$ minutes, the upward velocity is 0.73 m s^{-1}; at $t = 240$ minutes, the velocity is 0.81 m s^{-1}).

The propagation speed in experiment 2 is 13.5 m s^{-1} which represents a 33% increase over the speed of the disturbance in experiment 1. This increase can be attributed to both the greater stratification of the stable layer and the larger amplitude of the disturbance in experiment 2.

The numerical results also compare well with observations of the Morning Glory. The disturbance wavelength in experiment 2 is 9.0 km (compared to a wavelength of 10 km for the Glory on 4 October) and the propagation speed of 13.5 m s^{-1} compares to an observed speed of 11.2 m s^{-1} relative to the air at the ground.

The Scorer parameter in the region *downwind* of the leading jump has been plotted in Fig. 5. Also plotted are the individual terms $gB/(U - c)^2$ and $-U''/(U$

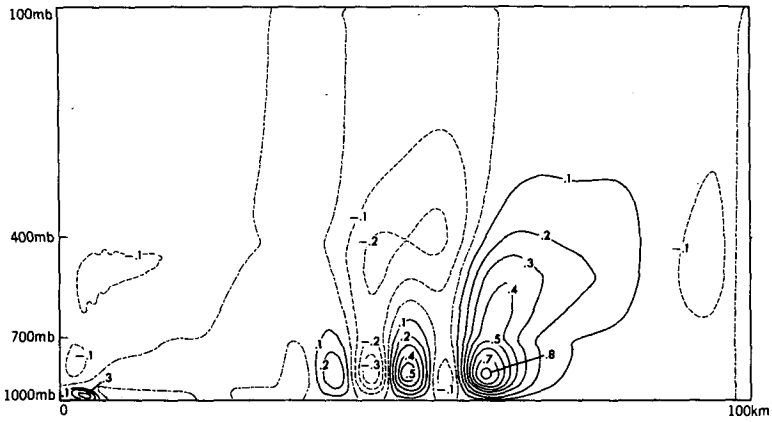

FIG. 4(a). Vertical velocity field for experiment 2 at $t = 240$ minutes. Note that the top pressure surface is 100 mb and that the pressure scale is contracted by a factor of 2 compared with Fig. 2. The damping layer is built up linearly from the 400 mb pressure surface.

$-c$). It is important to calculate these terms downwind of the bore as the flow profiles are significantly modified by the action of the bore. This is especially true for the curvature term $-U''/(U-c)$ which, as can be seen, is large near the ground—whereas in the upstream flow, there is no curvature in the wind profile near the ground.

At low levels, the Scorer parameter is large and positive, which is partly due to the strong stratification, but also due to the wind curvature produced at the top of the stable layer. Downwind of the bore, large forward velocities develop and produce a large degree of shear in the stable layer. The curvature term $-U''/(U-c)$ thus becomes important at the top of the stable layer since there is very little shear produced above this level. Higher up, l^2 changes sign, a result due to the curvature in the wind profile at the bottom of the westerly jet. Above this level, the strong westerly winds cause l^2 to be small and positive.

Also plotted in Fig. 5 is the square of the wavenumber k^2 for the wave at low levels. If $l^2 > k^2$, then the wave propagates upwards (Scorer, 1949); if not, the wave decays. As can be seen from Fig. 5, the wave is able to propagate up to about 800 mb. Above this level, the wind curvature and the strong westerly flow cause the wave to decay.

From Fig. 5a, it is clear that the curvature in the wind profile at the base of the jet (around 700 mb) will strongly trap waves propagating through this layer. This raises the question of the importance of the depth of this layer for wave trapping. The degree of trapping in a layer of depth H can be estimated in the following manner. We first assume that in this layer the curvature term $|U''/(U-c)|$ is much larger than both $gB/(U-c)^2$ and k^2. From Fig. 5, this is certainly true at the base of the jet in this high shear example, but may not be such a good approximation in the weak shear case examined later (experiment 3). Following Scorer (1949), the wave will then decay according to

$$w \propto \exp(-(k^2 - l^2)^{0.5} z) \approx \exp\left[-\left(\frac{U''}{U-c}\right)^{0.5} z\right].$$

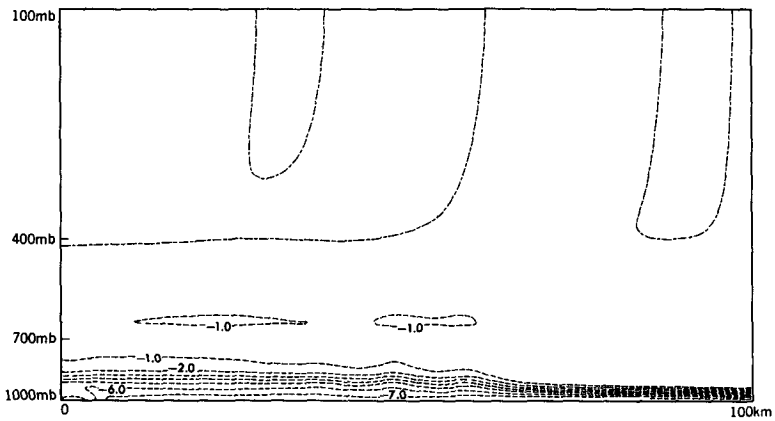

FIG. 4(b). As in 4a but for deviation potential temperature.

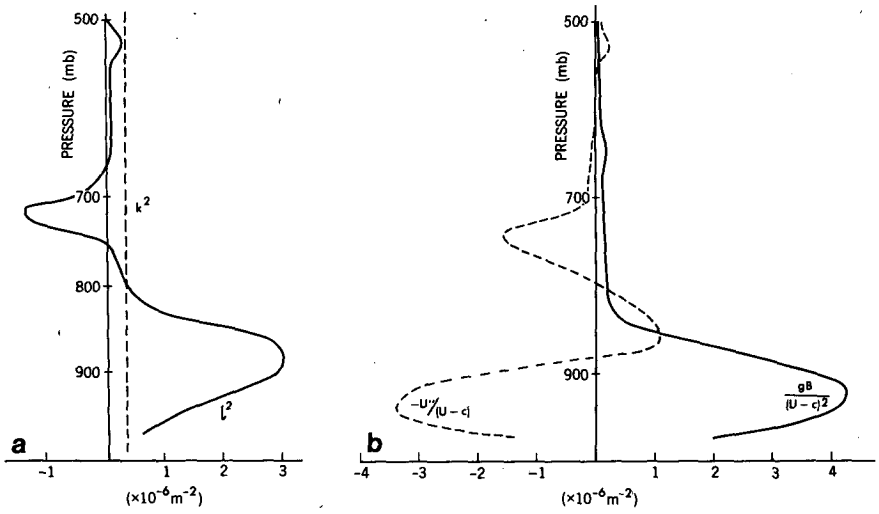

FIG. 5. (a) Scorer parameter downstream of the bore in experiment 2. Also plotted is the square of the dominant wavenumber k. (b) The individual terms $gB/(U-c)^2$ and $-U''/(U-c)$.

For simplicity, we assume that there is no shear below the layer; then if the shear at the top of the layer is U',

$$U'' \sim U'/H.$$

If we take the amplitude of the wave at the bottom of the layer to be unity, then at the top of the layer the amplitude will be,

$$w \approx \exp\left[-\left(\frac{U'H}{U_M - c}\right)^{0.5}\right],$$

where U_m is some mean wind in the layer.

It is clear from the above expression that for a *fixed* increase in shear, U', the amplitude reduction increases as the depth of the curvature layer increases. Thus, in the real atmosphere where the region of high curvature may be smoothed over a larger depth than in the numerical model, the trapping caused by this layer may be greater. However, it should be remembered that as the depth of the layer increases the assumption that the curvature term is much larger than the other two terms will eventually be violated.

3) WEAKER JETS

In the previous subsection (2), it was shown that the upward radiation of energy that occurs in an undular bore is reduced in the presence of opposing winds at upper levels. To examine this effect more quantitatively, the model was run with the same thermodynamic structure as before but with the upper winds reduced by 50%. (The jet velocity is now 16 m s^{-1} above 500 mb.)

In Fig. 6, the vertical velocity is shown at t = 190 min, experiment 3. First, a disturbance has propagated far ahead of the density current and can be seen interacting with the right-hand side of the domain. However, this is clearly not a trapped wave as the maximum

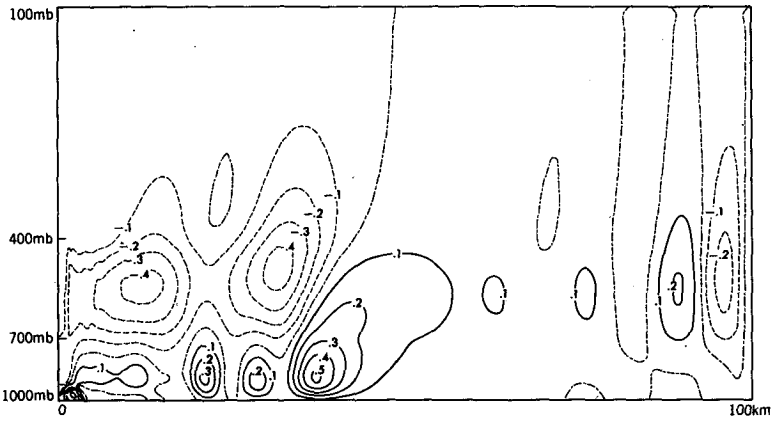

FIG. 6. Vertical velocity in experiment 3 (with reduced jet) at t = 190 minutes.

vertical velocity occurs somewhat above the stable layer.

Near the left-hand side of the domain, a wave at low-levels can be seen. Not surprisingly, the amplitude of the wave has been decreased by the weaker jet (vertical velocities being reduced by 25%). Furthermore, the upward radiation of energy has produced a large area above the stable layer with descending velocity of almost the same magnitude as in the trapped wave.

Another feature to note is that the wavelength of the trapped wave has been reduced (by 36%). This result can be best explained by referring to Fig. 7 in which the Scorer parameter downwind of the leading wave has been plotted. The weaker velocities and wind curvature in the jet have caused the Scorer parameter in this region to be increased compared with experiment 2. As the criterion for wavetrapping, $k^2 > l^2$, depends on the wavelength, the longer waves that were previously trapped by the jet have either been trapped less strongly or have been able to propagate into the upper levels of the domain (leaving the shorter wavelengths at low levels).

c. *The effects of moisture*

Perhaps the most striking feature of the Morning Glory is the wave clouds usually associated with the disturbance. Although "dry" Glorys have been recorded, they usually occur with one, two or more cloud bands.

The fact that dry disturbances have been observed suggests that moisture does not play a crucial role in the *formation* of the bore. However, moisture undoubtedly affects the structure of the wave through the release of latent heat. In the ascending branch of the wave, if condensation occurs, latent heat will be released and the buoyancy of the air increased. Conversely, as the air descends and evaporation occurs, the buoyancy decreases. If no precipitation occurs, then the net change of buoyancy during the process is zero. The fact that condensation has temporarily increased the buoyancy of the air might suggest that the amplitude of the wave should also increase. However, as will be seen, the inclusion of moisture has precisely the opposite effect.

1) THE INCLUSION OF MOISTURE IN THE MODEL

To allow for the presence of cloud in the model, two extra prognostic variables are solved for (see Miller and Pearce, 1974). These are q, water vapor content, and q_c, cloud water content (both in g kg^{-1} of moist air). After each timestep, the water vapor content is checked against the saturated value q_{sat} for the model temperature. If q exceeds q_{sat}, then q and the temperature are altered, subject to energy conservation, until the final vapor content is the saturated value for the final temperature. Conversely, if cloud exists in subsaturated air, then q_c is decreased until saturation occurs or until the cloud disappears.

Before examining the results from a simulation with moisture, it is important to note that the inclusion of moisture not only allows the possibility of cloud formation but also alters the effective stratification of the atmosphere. The reason for this is that moist air has a lower density than dry air at the same temperature and pressure or a greater temperature at the same density and pressure. This effect is usually taken into account by defining a new temperature, the virtual potential temperature:

$$\theta_v = \theta(1 + 0.61q),$$

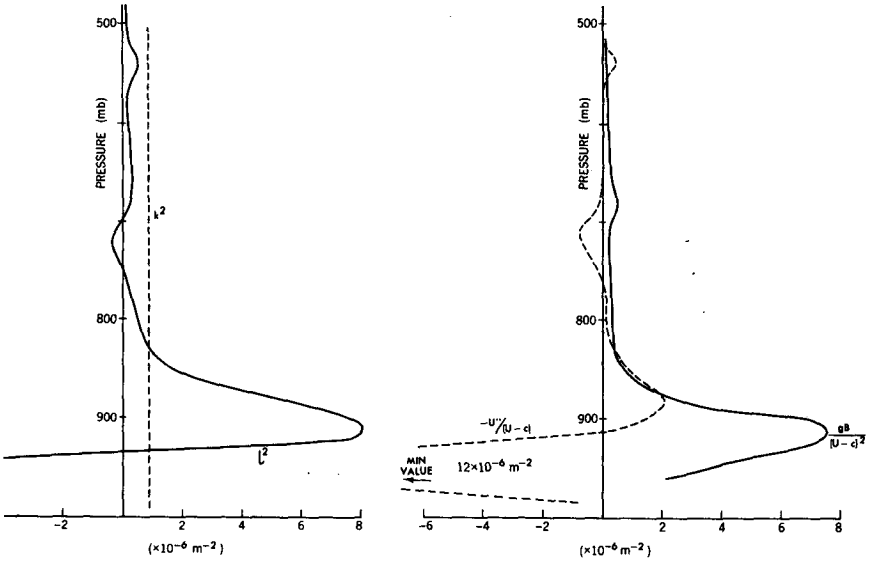

FIG. 7(a), (b). As in Figs. 5a, b except for experiment 3 with a weaker jet. Note that the horizontal scale has been contracted by a factor of 2.

where q is the water vapor content in g kg^{-1}. Now as the water vapor content usually decreases upwards, θ_v does not increase upwards as rapidly as θ and hence the atmosphere is less stable. For this reason, it is difficult to make model comparisons between dry and moist atmospheres. However, as will be shown, this difficulty can be circumvented by comparing two moist simulations, one of which has the condensation subroutines "turned off" (so that the mixing ratio can become greater than q_{sat}).

Measurements taken at Burketown during a Morning Glory observational experiment show that the stable layer is very moist [the relative humidity at the ground on 4 October 1979 was 96% (Clarke et al., 1981)]. Above the stable layer, the relative humidities observed are of the order of 30 to 40% which are typical values for a tropical atmosphere near the end of the dry season.

In the model, the moisture profile is simplified to two linear profiles of relative humidity. At the ground, the relative humidity is denoted as Q_{RAT2} and decreases linearly to Q_{RAT1} at the top of the stable layer. In the upper layer, the relative humidity decreases linearly to $Q_{RAT1}/2$ at the top of the model.

The following humidity values were taken for the first simulation:

$$Q_{RAT1} = 0.55,$$

$$Q_{RAT2} = 0.96.$$

The air at the top of the stable layer is slightly more moist than usually observed. This allows deeper clouds to form and makes it easier to study the effects of condensation. The potential temperature and velocity structure are the same as in experiment 2.

2) MODEL RESULTS

Several trial simulations were necessary before individual wave clouds, similar to those in the Morning Glory, could be produced. To obtain wave clouds, the moist air near the surface needs to be lifted above the condensation level but not above the level where the air becomes positively buoyant; otherwise free convection will set in. Also, when condensation occurs, it is necessary for the air to be allowed to descend, otherwise individual wave clouds will not appear. This was a difficulty with the first experiments, in which the density current was allowed to propagate into the domain for the duration of the experiment. In these experiments, a stronger density current (with $\Delta p_I = 75$ mb and $\tilde{\theta}'/\theta_0 = 0.12$; see Fig. 1) was needed to produce condensation. However, the strength of the density current resulted in the current propagating too quickly for any disturbance to move ahead.

These early experiments made it clear that to obtain reasonably large wave clouds propagating *ahead* of the density current it is necessary for the current to decelerate after it has interacted with the stable layer. Furthermore, in the real system in northern Queensland, deceleration of the sea breeze is to be expected, as the thermal forcing of the breeze ceases during the night.

For this reason, an experiment was run in which the velocity prescribed at the density current inflow was decreased monotonically after the current had interacted with the stable layer. To reduce the inflow velocity, a similar procedure is used to that implemented at the start of the simulation to increase the inflow (see CM, section 2).

In Fig. 8, the cloud and vertical velocity fields at $t = 135$ minutes and 216 minutes are shown (experiment 4). Comparing Figs. 4 and 8, it can be seen that the vertical velocities have increased by a factor of 2. This increase can be partly attributed to the stronger density current used to initiate the disturbance but also to the decrease in stratification above the stable layer that moisture has caused. In this layer, the stratification based on the virtual potential temperature is

$$B = \frac{1}{\theta_v}\frac{\partial \theta_v}{\partial z} = 3 \times 10^{-6}\ \text{m}^{-1},$$

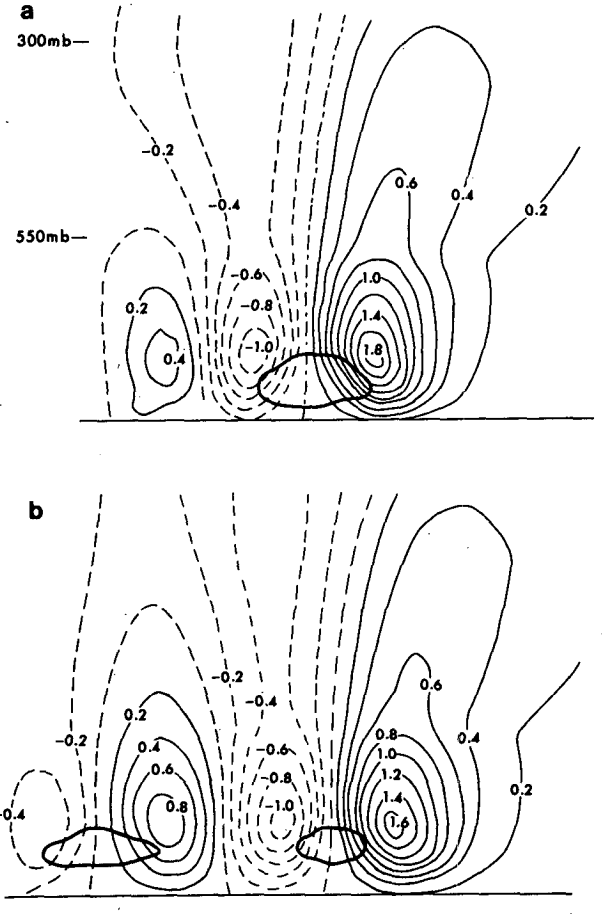

FIG. 8. (a) Vertical velocity and cloud fields for experiment 4 at $t = 135$ min. Heavy line is the 0.01 g kg^{-1} contour of q_c. Both horizontal and vertical scales are expanded by a factor of 2 compared with Figs. 4 and 6. (b) As in (a) except at $t = 216$ minutes. The density current is approximately 16 km behind the second cloud.

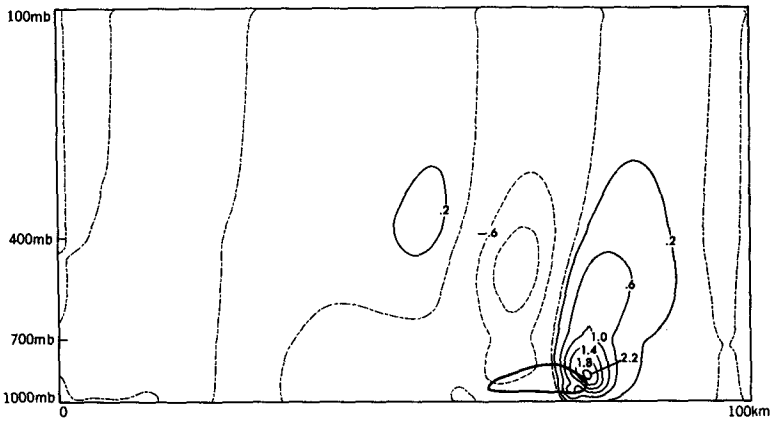

FIG. 9(a). Vertical velocity field in experiment 5 at $t = 216$ minutes. Heavy line is the 0.01 g kg^{-1} contour of q_c.

which represents a 40% decrease in stratification compared with the dry simulation. This reduction in stratification results in a greater trapping of energy in the region above the stable layer and a consequent increase in amplitude at low levels.

As can be seen from Fig. 8, two wave clouds have formed after 216 minutes. These clouds form in the region between the ascending and descending branches of the wave where the air in the stable layer is lifted to its greatest height, i.e., in the crest of the wave.

The cloud depths obtained in experiment 4 are somewhat less than those observed. In the numerical simulation, the pressure difference between cloud top and bottom is 60 mb ($\approx$600 m) whereas on 4 October 1979, the first cloud had a depth $\approx$ 1200 m. To obtain these deeper clouds, it would be necessary for a considerably stronger density current to interact with the stable layer. However, the timescale for bore development is then substantially increased and the consequent increase in computer time makes it expensive (computationally) to study these stronger disturbances.

3) COMPARISON WITH A DRY ATMOSPHERE

As mentioned earlier, the simplest method of examining the effects of condensation is to run two moist simulations and to disallow in one the possibility of cloud formation.

Experiment 4 was repeated with the cloud routine switched off. Because of the relatively small amounts of cloud in the experiment, the changes that occur are slight. However, the presence of cloud causes a small decrease in the wave amplitude. With cloud the maximum vertical velocity is reduced by approximately 5%.

To explore this behavior further, an experiment was run with a stronger density current in order to produce deeper clouds (experiment 5). The density current parameters were increased to $\tilde{\theta}'/\theta_0 = 0.015$ and $\Delta p_I = 90$ mb. At $t = 216$ minutes, one wave has formed and this is shown in the vertical velocity field, Fig. 9. (As already stated, a considerable amount of computer time would be needed to simulate the full development of the bore.)

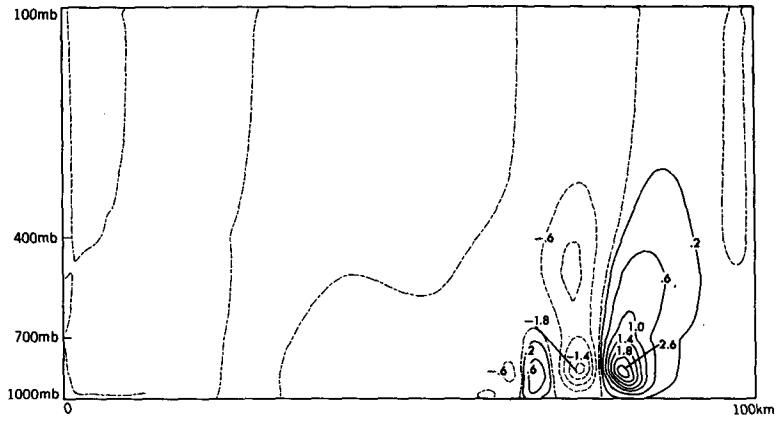

FIG. 9(b). As in Fig. 9(a) except cloud is not allowed to form. Note that with cloud the disturbance is weaker at low levels, has a longer wavelength and more energy at upper levels.

The cloud in this wave has a depth of ≈ 1 km with a maximum cloud water content of ≈ 1 g kg^{-1}.

In Fig. 9b, the vertical velocity field for the same experiment, but without cloud, is depicted. As can be seen, the vertical velocities are reduced when cloud is present, in this case by 20%. This at first surprising result has been noted by several previous authors (see, for example, Barcilon et al., 1979; Smith and Lin, 1982). The explanation put forward by these authors is that condensation decreases the stability of the atmosphere. In a moist flow, it is no longer potential temperature that is conserved by the fluid, but equivalent potential temperature $\theta_E = \theta \exp(L_c q_{SAT}/C_p T)$ and this decreases less rapidly in the stable layer. In the present simulation, the potential temperature difference across the stable layer is 10°C, while the difference in equivalent potential temperature is only 6°C. Note that the effective difference is somewhere between these two values, since only part of the stable layer is cloudy.

As the effective stratification in the stable layer is reduced, less energy can be trapped at low levels. More energy is transmitted into the upper atmosphere, and this can be seen by comparing Fig. 9a and 9b. In the cloudy experiment, the downward velocity in the middle of the atmosphere has been increased by 20%.

The escape of energy upwards is compounded by the increase in wavelength that occurs when condensation is included. In the noncondensation run, the wavelength is 12.7 km, whereas with condensation, the wavelength is 20.1 km. This increase can be explained in the following manner. There is little difference in the speed of the bore, 15.1 m s^{-1} for noncondensation and 14.9 m s^{-1} with condensation. As the speed of the bore depends solely on the difference in height of the stable layer between regions far upstream and downstream of the bore (see Benjamin and Lighthill, 1954), it is not altered if a cloud forms and completely evaporates downstream.

However, the wave speed *is* affected by condensation, since it reduces the effective stability through which the wave propagates. Now the horizontal phase velocity of internal gravity waves in a nonrotating system is given by

$$C_x = \frac{N}{(k^2 + m^2)^{0.5}},$$

where k and m are the horizontal and vertical wavenumbers respectively. Hence the phase speed increases as the horizontal wavelength increases (noting that the vertical wavenumber is fixed by the trapping characteristics of the atmosphere). Thus, a wave with condensation (in which the effective N is reduced) must increase its wavelength in order that it propagate at the same speed as a dry wave.

3. Discussion and conclusion

The present research has indicated the following necessary conditions for undular bore behavior:

1) a generating mechanism such as a sea breeze, thunderstorm outflow or cold front;

2) a Scorer parameter decreasing with height. This can be achieved by the presence of
   a) a strongly stratified stable layer at the ground,
   b) weak stratification above the stable layer, and
   c) strong winds opposing the wave motion at upper levels.

For the formation of stable wave clouds, it is necessary to have

3) high relative humidity in the stable layer, drier above.

In section 2b, it was shown that the westerly jet that often exists over northern Queensland assists in the trapping of energy in disturbances that propagate from the east. However, Morning Glory disturbances have also been observed to propagate from a southerly direction and for these disturbances the upper-level wind in a ground-based reference frame is *perpendicular* to the direction of motion. Two comments will be made about the trapping of energy in these disturbances. First, the lifetime of southerly disturbances tends to be shorter than that of northeasterly disturbances (R. H. Clarke, personal communication, 1984). One possible explanation for this is that southerly disturbances in general are less strongly trapped in the vertical and that upward radiation of energy is limiting their lifetime.

Secondly, disturbances from the south tend to have a greater propagation speed than those from the northeast (17 m s^{-1} on 10 December 1980, 15 m s^{-1} on 10 September 1980—see Smith et al., 1982, and 18.4 m s^{-1} on 26 October 1984, unpublished). This increased wavespeed is most likely due to the fact that the winds below 4 km are usually southeasterly and thus assist the propagation of southerly disturbances. Above the southeasterly trades in the region where the flow turns westerly, the wind speed, in a frame reference in which the wave is at rest, will be increased and consequently the Scorer parameter reduced. Furthermore, the wind curvature in the region between the southeasterly and westerly flow is such as to assist wave trapping.

The author's attention has recently been drawn to a related work by Clarke (1984) on interacting sea breezes. Briefly, a hydrostatic sea breeze model was run with *two* coastlines separated by a distance of 440 km which is an average width of Cape York Peninsula where northeasterly disturbances are believed to form. The numerical model was run with various cross-peninsula winds which were constant with height for each case. After a day of solar heating, the sea breezes would meet at about midnight and, depending on the value of the cross-peninsula wind, one or two bores would form. For low values of the background wind, ~ 1 m s^{-1}, two bores moving in opposite directions would form; for higher winds only the bore moving in the direction of the background wind would form.

The bores that were produced were not followed by substantial gravity waves, and this Clarke attributed to

the neglect of the nonhydrostatic terms in the equation of motion.

What is of particular interest in this work is the structure and long-term progress of the bores that are created. Clarke uses a similar potential temperature profile to that used in the present study except that he includes an inversion of 5°C at approximately 2700 m. He finds that the vertical velocity decays rapidly in the region of the inversion, but then increases above that height (see Fig. 16b). Clearly, some energy is being reflected off the inversion layer and hence trapped in the lower layers of the atmosphere and some is leaking through.

Related to this observation is the long-term behavior of the bore. Clarke finds that his simulated bores decay with time; there is an approximately 33% decrease in amplitude over 3 h for the case where the background wind is equal to 5 m s^{-1} (Table 4, Clarke, 1984). This decay, with time, is most likely due to the upward radiation of energy by the gravity waves above the inversion. Note that the wave trapping mechanism proposed in the present work cannot operate in Clarke's model as there is no shear in the environment. However, despite this leakage of energy, significant amplitudes are produced (although in general, less than those observed), suggesting that the inversion at around 3 km is important in the dynamics of the Morning Glory. It is planned to investigate the relative importance of inversions and opposing shears in a future work.

If condensation occurs, the numerical results in the present work have shown that the disturbance amplitude is reduced. This somewhat surprising result has been noted by a number of authors; however, it does not seem to be widely recognized (see, for example, Clarke et al., 1981). The numerical simulations have also shown that cloud tends to increase the wavelength of the disturbance.

Acknowledgments. A significant portion of this work was completed while the author was a graduate student at Imperial College, University of London. The author would like to thank Drs. M. Miller and J. Green for their helpful comments. The clarifying comments made by Drs. I. Orlanski and F. Lipps, the patience and skill exhibited by J. Callan in typing the manuscript and the GFDL graphics support staff are also acknowledged. The author would also like to thank Dr. R. Clarke for interest in this research and for several illuminating discussions. Finally the financial support given by the Geophysical Fluid Dynamics Program at Princeton University under NOAA Grant NA84-EAD00057 is gratefully acknowledged.

REFERENCES

Barcilon, A., C. Jensen and P. A. Drazin, 1979: On the two-dimensional hydrostatic flow of a stream of moist air over a mountain range. *Geophys. Astrophys. Fluid Dynamics,* **13,** 125–140.

Benjamin, T. B., and M. J. Lighthill, 1954: On cnoidal waves and bores. *Proc. Roy. Soc.,* **A224,** 448–460.

Clarke, R. H., 1984: Colliding sea-breezes and the creation of internal atmospheric bore waves: Two-dimensional numerical studies. *Aust. Meteor. Mag.,* **32,** 207–226.

——, R. K. Smith and D. Reid, 1981: The Morning Glory of the Gulf of Carpentaria. An atmospheric undular bore. *Mon. Wea. Rev.,* **109,** 1726–1750.

Crook, N. A., and M. J. Miller, 1985: A numerical and analytical study of atmospheric undular bores. *Quart. J. Roy. Meteor. Soc.,* **111,** 225–242.

Eliassen, A., and E. Palm, 1961: On the transfer of energy in stationary mountain waves. *J. Geophys. Publ.,* **22,** 1–23.

Miller, M. J., and R. P. Pearce, 1974: A three-dimensional primitive equation model of cumulonimbus convection. *Quart. J. Roy. Meteor. Soc.,* **100,** 133–154.

Scorer, R. S., 1949: Theory of waves in the lee of mountains. *Quart. J. Roy. Meteor. Soc.,* **75,** 41–56.

Smith, R. B., and Y. L. Lin, 1982: The addition of heat to a stratified airstream with application to the dynamics of orographic rain. *Quart. J. Roy. Meteor. Soc.,* **108,** 353–378.

Smith, R. K., and B. Morton, 1984: An observational study of north-easterly "morning glory" wind surges. *Aust. Meteor. Mag.,* **32,** 155–175.

——, N. Crook and G. Roff, 1982: The Morning Glory: An extraordinary atmospheric undular bore. *Quart. J. Roy. Meteor. Soc.,* **108,** 937–956.